Journal of Molecular Graphics and Modelling 92 (2019) 216–226

Contents lists available at ScienceDirect

Journal of Molecular Graphics and Modelling

journal homepage: www.elsevier.com/locate/JMGM

Deciphering the structural basis for glucocorticoid resistance caused by missense mutations in the ligand binding domain of glucocorticoid receptor

L.L.S. Monteiro [a], O.L. Franco [a, b, d], S.A. Alencar [a], W.F. Porto [c, d, *]

[a] Programa de Pós-Graduação Em Ciências Genômicas e Biotecnologia, Universidade Católica de Brasília, Brasília, DF, Brazil
[b] Centro de Análises Proteômicas e Bioquímicas, Pós-Graduação Em Ciências Genômicas e Biotecnologia, Universidade Católica de Brasília, Brasília, DF, Brazil
[c] Porto Reports, Brasília, DF, Brazil
[d] S-Inova Biotech, Pós-Graduação Em Biotecnologia, Universidade Católica Dom Bosco, Campo Grande, MS, Brazil

ARTICLE INFO

Article history:
Received 11 April 2019
Received in revised form
1 July 2019
Accepted 31 July 2019
Available online 1 August 2019

Keywords:
NR3C1
SNVs
Structure-function relationship
Molecular docking
Molecular dynamics

ABSTRACT

The glucocorticoid resistance hereditary condition may emerge from the occurrence of point mutations in the glucocorticoid receptor (GR), which could impair its functionality. Because the main feature of such pathology is the resistance of the hypothalamic-pituitary-adrenal axis to the hormone cortisol, we used the GR ligand binding domain three-dimensional structure to perform computational analysis for eight variants known to cause this clinical condition (I559 N, V571A, D641V, G679S, F737L, I747 M, L753F and L773P), aiming to understand, on the atom scale, how they cause glucocorticoid resistance. We observed that the mutations generated a reduced affinity to cortisol and they alter some loop conformations, which could be a consequence from changes in protein motion, which in turn could result from the reduced stability of mutant GR structures. Therefore, the analyzed mutations compromise the GR ligand binding domain structure and cortisol binding, which could characterize the glucocorticoid resistance phenotype.

1. Introduction

Glucocorticoid resistance is characterized as a rare condition that can be inherited or acquired, affecting the whole body or only certain tissues. This disease consists of a resistance of the hypothalamus-pituitary-adrenal axis (HPA) to the cortisol hormone, which in turn is secreted in greater amounts as a compensation mechanism [1]. The occurrence of altered glucocorticoid receptors (GRs) in HPA axis cells may result in the generalized glucocorticoid resistance form [2]. Besides, the cortisol hormone is responsible for some behaviors; therefore, the clinical condition of glucocorticoid resistance has been related to major depression [3].

The *NR3C1* gene encodes GR protein, which promotes cortisol transport to the cell nucleus, where it exerts regulatory activity [4]. GR activity can be measured by the dexamethasone-binding test, which allows a decrease in GR affinity for the ligand to be determined and compared to a control group. After a diagnosis of reduced activity, the next step comprises sequencing the receptor gene to search for mutations that may be impairing its function [5].

The receptor has two isoforms derived from alternative splicing in *NR3C1* gene exon 9, where only the α isoform is biologically active [6]. GRα is synthesized in almost all body tissues and consists of 777 amino acids, functioning as a binding-dependent transcription factor [7]. In ligand absence, GR is in the cell cytoplasm, comprising a multiprotein complex formed by the receptor polypeptide and heat shock proteins (HSPs). After cortisol binding, HSPs dissociate from GR. The receptor-hormone complex binds to another identical complex to form the homodimer that will act on the cell nucleus (Fig. 1).

GR has three domains called (i) the DNA-binding domain (DBD), which also comprises the protein dimerization site, being located in the central portion; (ii) the ligand-binding domain (LBD), located at the C-terminal, responsible for binding of the protein to glucocorticoids forming the receptor-hormone complex; and (iii) the transactivation domain, divided into two activation function (AF)

* Corresponding author. S-Inova Biotech, Pós-Graduação Em Biotecnologia, Universidade Católica Dom Bosco, Campo Grande, MS, Brazil.
E-mail address: williamfp7@yahoo.com.br (W.F. Porto).

https://doi.org/10.1016/j.jmgm.2019.07.020
1093-3263/

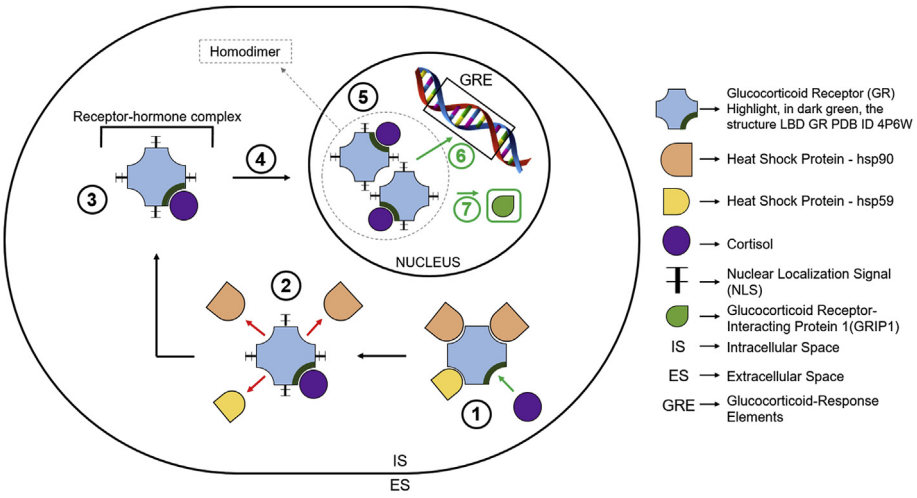

Fig. 1. Schematized action mechanism of glucocorticoid receptor (GR). The (1) receptor remains inactive in the cytoplasm associated with heat shock proteins (HSPs) that provide glucocorticoid binding, in addition to inactivating the nuclear localization signals (NLSs) of the GR. After (2) cortisol binding, the HSPs proteins dissociate from the receptor and the NLSs are activated. The (3) receptor-hormone complex is formed and (4) translocated to the nucleus by means of the NLSs, and (5) combines with another GR complex composing a homodimer, which (6) binds to glucocorticoid-response elements in DNA and (7) interacts with GRIP1 transcription factor for gene expression regulation.

subdomains located at the N-terminal (AF-1) and C-terminal (AF-2). AF-1 and AF-2 subdomains of GR directly interact with glucocorticoid receptor-interacting protein 1 (GRIP1), a transcription factor that allows transcriptional activity and gene regulation independent of receptor binding to glucocorticoid response elements (GREs) in DNA [1,6,8].

GR activity could be altered by specific amino acid substitutions, resulting from single nucleotide polymorphisms (SNPs) present in coding regions of the *NR3C1* gene [1]. Alterations may occur in the different steps of the GR action mechanism, as shown in Fig. 1. These changes in GR cause different glucocorticoid resistance phenotypes. However, GR structural modifications that could impair its activity are not well characterized. In this context, *in silico* structural analyses, including molecular docking and molecular dynamics, can give some insights and evaluate structural changes.

Molecular docking analysis can be applied to a number of structural bioinformatics problems involved in the prediction of protein function in studies that evaluate the effect of mutations such as deletions, insertions and/or point mutations [9]. Some of its applications involve the analysis of the structural effect of SNPs on protein-drug complexes for resistance or pharmacological sensitivity studies [10], as well as in analyses between receptors and endogenous hormones, such as the study of point mutations in the growth hormone receptor [11]. For a more detailed evaluation of structural modifications, molecular dynamics is performed to analyze the changes that occur with the receptor-ligand complex.

Molecular dynamics (MD) simulations provide the evaluation of the conformation of three-dimensional protein structures for a given period of time in simulated environments [12], thus providing details of individual atomic motions in the protein chain and also the observation and evaluation of changes in physicochemical properties and interactions [13,14]. In this context, MD is widely used in analyses of potentially deleterious SNPs from proteins involved in cancer, such as aurora-A kinase [14,15], mitochondrial NADH dehydrogenase [16], RAS-related C3 botulinum toxin substrate 1 [17], proliferating nuclear antigen [18] and P53 [19]; and also missense SNPs from proteins involved in a number of different diseases, such as guanylin peptides [20–22], α- and β-defensins [23,24], apolipoprotein E [13], phospholipase A2-IIA [25], vitamin D receptor [26] and pyrroline-5-carboxylate reductase [27].

Here, we evaluated the structural effect of pathological missense SNPs on the *NR3C1* gene, in order to understand how they actually cause glucocorticoid resistance. The SNPs were obtained from the dbSNP database and assessed by means of polymorphism prediction tools and analysis of changes in the glucocorticoid receptor structure of the glucocorticoid resistance mutations using molecular docking and molecular dynamics simulation.

2. Material and methods

2.1. Datasets

The *NR3C1* gene information was obtained from the National Center for Biotechnology Information (NCBI), in the NCBI Gene database (Gene ID 2908). The glucocorticoid receptor protein sequence in the FASTA format (NCBI Accession: NP 000167.1) was retrieved from the NCBI Protein database. The Ligand Binding Domain (LBD) structures were collected from the Protein Data Bank (PDB) (PDB ID 4P6W; PDB ID 4P6X). Data on missense SNPs were acquired through the Variation Viewer website (https://www.ncbi.nlm.nih.gov/variation/view/), accessing the database of Single Nucleotide Polymorphisms (dbSNP build 151) using the single nucleotide variant, missense variant and pathogenic filters, respectively. We selected pathological SNPs that were covered by the LBD domain.

2.2. Evolutionary conservation analysis

Consurf [28] is a tool that estimates the evolutionary conservation of amino acid positions in a protein sequence based on homologous sequences. The amino acid conservation is presented in a colorimetric scale ranging from the most variable position (number 1, in blue) to the most conserved (number 9, in red) [29]. Using the protein sequence for the Ligand Binding Domain (LBD) of the glucocorticoid receptor (PDB ID 4P6W) and ConSurf in the ConSeq mode, a search for homologous sequences was made using the CSI-BLAST algorithm (3 interactions and e-value equal to 0.0001) against the UNIREF-90 protein database [30,31]. The maximum number of homologs close to the query sequence was set to 150, and the minimum and maximum percentage of ID between the sequences was set to 35 and 95, respectively. Multiple sequence alignment and conservative score calculation methods were set as

default (MAFFT-L–INS–i and Bayesian).

2.3. Prediction of structural stability of pathological missense SNPs

In order to analyze the missense SNPs selected with respect to the free energy difference (ΔΔG), we used the prediction programs PoPMuSiC (https://soft.dezyme.com) [32], Site Director Mutator (SDM - http://marid.bioc.cam.ac.uk/sdm2/) [33], and FoldX (http://foldxsuite.crg.eu/) [34]. For the analysis of the melting temperature difference (ΔΔT), the programs HoTMuSiC (https://soft.dezyme.com) [35] and SNPMuSiC (https://soft.dezyme.com) [36] were used. All programs use a PDB file and a list of mutations as the input. We used the LBD structure (PDB ID 4P6W, chain A) and the programs were used in their default settings. The concordance between the predictors was demonstrated by the coefficient of determination (R squared).

2.4. Molecular modeling

One hundred molecular models for each variant, without cortisol ligand, were constructed by comparative molecular modeling by means of MODELLER 9.19 [37], using the LBD structure of the glucocorticoid receptor (PDB ID 4P6W, chain A; resolution 1.95 Å, comprising the residues 526 to 777). The models were constructed using the default methods of automodel and environ classes from MODELLER. The final models were selected according to the discrete optimized protein energy score (DOPE score). This score assesses the energy of the models and indicates the best probable structures. The best models were evaluated by means of PROSA II [38] and PROCHECK [39]. PROCHECK checks the stereochemical quality of a protein structure by means of the Ramachandran plot, where good quality models are expected to have more than 90% of amino acid residues in most favored and additional allowed regions, while PROSA II indicates the fold quality. Structural visualization was done in PyMOL (http://www.pymol.org).

2.5. Molecular docking

The theoretical molecular docking studies were performed using AutoDock Vina [40] and Autodock Tools [41]. The Autodock Vina plug-in from PyMOL was used to set the system. The cortisol structure was obtained from the ligand-binding domain of the glucocorticoid receptor (PDB ID 4P6X, chain A; resolution 2.5 Å) [42]. Then the best molecular model for wild-type and each variant were aligned to 4P6X, in order to set all models in the same position, allowing a single grid box set up for all models. The grid box was configured to allow the interaction of the cortisol molecule with the LBD. Initially, the grid box center was defined according to the cortisol position, which corresponds to coordinates 4.37, 32.25 and −7.22 from X, Y and Z axes, respectively. Then the grid was resized to 30 $Å^3$. On the receptor pdbqt files, no flexible side chains were set, avoiding unnatural positions, since the binding residues are known from the LBD-cortisol complex (PDB ID 4P6X). On the ligand pdbqt file, no flexibility was allowed as the cortisol structure is constrained by their rings. Receptor and ligand files were generated using Autodock Tools under the default parameters. Then, one hundred independent replicates, using different seeds, were performed for wild-type and variant structures. The theoretical affinity comparisons between cortisol coupled to LBD and the structural models with the SNPs were carried out by means of the evaluation of the energy given in $kcal.mol^{-1}$. A two-sided Wilcoxon-Mann-Whitney non-parametric test was applied to verify the differences between the wild-type and variants' binding energy, with a critical value of 0.05. The statistical analyses were done by means of the R package for statistical computing (http://www.r-project.org).

2.6. Molecular dynamics simulations

The molecular dynamics simulations were done according to Kumar and Purohit (2014) with minor modifications. The ensembles were carried out in water environment, using the Single Point Charge water model [43], under ionic strength conditions (0.2 M NaCl), as explicit salt ions are important for protein stability [44]. The analyses were performed by using the GROMOS96 43A1 force field and computational package GROMACS 4.6 [45]. The dynamics used the GR wild-type and variants' three-dimensional models as initial structures, immersed in water, in cubic boxes with a minimum distance of 8 Å between the proteins and the edges of the boxes. The topology of the cortisol molecule was generated by the PRODRG tool, allowing chirality and full charges; no energy minimization was performed [46]. Additional counter ions were also inserted into the complexes in order to neutralize the system charge. Geometry of water molecules was constrained by using the SETTLE algorithm [47]. All atom bond lengths were linked by using the LINCS algorithm [48]. Electrostatic corrections were made by Particle Mesh Ewald algorithm [49], with a cut-off radius of 1.4 nm in order to minimize the computational time. The same cut-off radius was also used for van der Waals interactions. The neighbor searching was done using the Verlet cutoff scheme. The complete system was then submitted to an energy minimization process using 50,000 steepest descent algorithm iterations. After that, the system temperature was normalized to 310 K for 100 ps, using the velocity rescaling thermostat (NVT ensemble). Then the system pressure was normalized to 1 bar for 100 ps, using the Parrinello-Rahman barostat (NPT ensemble). The systems with minimized energy, balanced temperature and pressure were simulated for 200 ns by using the leap-frog algorithm.

2.7. Analyses of molecular dynamics trajectories

Molecular dynamics simulations were analyzed by means of the backbone root mean square deviation (RMSD), radius of gyration (GR) and solvent accessible surface area (SASA) using the g_rms, g_gyrate and g_sas functions of the GROMACS [45], respectively. For essential dynamics analysis, the main chain of wild-type and variants' protein trajectories was concatenated for general visualization of protein movement. This analysis extracts the protein motions and splits them in different components according to the degree of movement, being the 1^{st} component the largest class of motion for such structure, the second component is the 2^{nd} largest class and so on. This analysis allows quantifying and understanding the most fundamental motions of a given protein. Essential dynamics analysis was done using the g_covar and g_anaeig utilities. The number of hydrogen bonds between the cortisol molecule and the GR protein pocket residues Leu^{563}, Asn^{564}, Gln^{570}, Arg^{611} and Thr^{739} was analyzed using g_hbond, also from GROMACS package. The wild-type structure and a 200 ns snapshot of each mutant receptor were compared by means of the RMSD and TM-Score [50], where TM-Scores above 0.5 indicate that the two structures share the same fold [51].

3. Results

3.1. Pathological single nucleotide polymorphisms (SNPs) in NR3C1 gene

The *NR3C1* gene has 20.298 SNPs cataloged in dbSNP (build 151). The selection of the polymorphisms that caused glucocorticoid

resistance was done through screening pathological single nucleotide variations of missense type, totaling nine SNPs, and of these, eight SNPs were selected for analysis (Table 1). These polymorphisms are found in the Ligand-Biding Domain (LBD) and cause glucocorticoid resistance. The ninth SNP corresponding to the R477H mutation was excluded because it is not covered by the LBD domain.

3.2. The pathological character is independent of amino acid conservation

The conservation analysis of the GR LBD domain structure shows small regions of highly conserved amino acids at the beginning and at the end of the domain (Fig. 2). The eight evaluated mutations that cause resistance to glucocorticoids are mostly in conserved positions, especially the G679S mutation, which is in a position of higher conservation value. The L773P and D641V mutations are the only ones that are in variable conservation positions in the structure. The I559 N mutation is in an average conservation region.

3.3. The majority of pathological mutations destabilizes the GR LBD structure

For information on possible stability changes that mutations might cause in the GR LBD structure, pathological SNPs were subjected to prediction methodologies based on three-dimensional structure. Table S1 shows the results of the programs (PoPMuSiC, HoTMuSiC, SNPMuSiC, SDM and FoldX) used in the analysis of mutation effects. Overall, the programs presented a good pairwise correlation (Fig. 1). Direct and indirect correlations depend on how each pair of programs treats deleterious results. Positive values for PoPMuSiC and SNPMuSiC suggest deleterious effects on the I559 N, V751A, D641V, G679S, F737L, I747 M, L753F mutations in the protein structure, as well as negative values observed in the HoTMuSiC and SDM predictors, while the FoldX tool predicts deleterious mutations with a score above 0.5. Six out of eight mutations destabilize the GR LBD structure, with exception of D641V and L773P mutations, which could lead to the stabilization of the protein structure of the GR, according to the predicted values in three out of five programs used.

3.4. Ligand-binding domain GR model

By means of MODELLER, the wild-type and variant structures were obtained, as shown in Fig. 3. The GR LBD domain is composed of 11 α-helices and 4 β-strands. Pathological mutations occur in a diversified way in the domain structure, as indicated in Table 1.

3.5. Overall, mutations reduce the affinity between receptor and cortisol

The LBD-cortisol complex structure (PDB ID 4P6X, chain A) was used as the reference structure to molecular docking analyses in order to evaluate the hormone binding energy alterations caused by the missense mutations. Due to the rigid body configurations for docking, all structures kept the same binding residues from the reference structure: Leu^{563}, Asn^{564}, Gln^{570}, Arg^{611} and Thr^{739} (data not shown). Fig. 4 shows the binding energy obtained between the pathological SNPs tested compared to wild-type. The L753F mutation reached the energy value of -10.8 kcal mol^{-1} compared to wild-type, which was -10.6 kcal mol^{-1}, showing that cortisol could have higher affinity for GR L753F than for the wild-type structure. The other mutations may cause a decrease in affinity between

Table 1
Pathological mutations, their structural location and functional changes in GR protein action mechanism.

SNP rs ID	Mutation	Structural location	Receptor functionality changes	Reference
rs104893909:T→A	p.I559 N	α-Helix 3	Low Ligand binding affinity Low Transcriptional activity Delayed nuclear translocation Abnormal interaction with co-activator GRIP1	[1,6,52,53]
rs104893911:T→C	p.V571A	α-Helix 3	Low Ligand binding affinity Low Transcriptional activity Delayed nuclear translocation Abnormal interaction with co-activator GRIP1	[5,6]
rs104893908:A→T	p.D641V	α-Helix 7	Low Ligand binding affinity Low Transcriptional activity Delayed nuclear translocation Abnormal interaction with co-activator GRIP1	[6,54]
rs104893914:G→A	p.G679S	Loop between α-helices 8 and 9	Low Ligand binding affinity Low Transcriptional activity Delayed nuclear translocation No interaction with AF-2 subdomain Abnormal interaction with co-activator GRIP1	[52,55]
rs121909727:T→C	p.F737L	α-Helix 11	Low Ligand binding affinity Low Transcriptional activity Delayed nuclear translocation Abnormal interaction with co-activator GRIP1	[56]
rs104893910:T→G	p.I747 M	Loop between α-helices 11 and AF-2	Low Ligand binding affinity Low Transcriptional activity Slight delayed nuclear translocation Small interaction with AF-2 subdomain Abnormal interaction with co-activator GRIP1	[6,57]
rs121909726:A→T	p.L753F	α-Helix AF-2	Low Transcriptional activity Delayed nuclear translocation Receptor-hormone complex dissociation	[58–61]
rs104893912:T→C	p.L773P	C-terminal region (downstream of α-helix AF-2)	Low Ligand binding affinity Low Transcriptional activity Delayed nuclear translocation Abnormal interaction with co-activator GRIP1	[1]

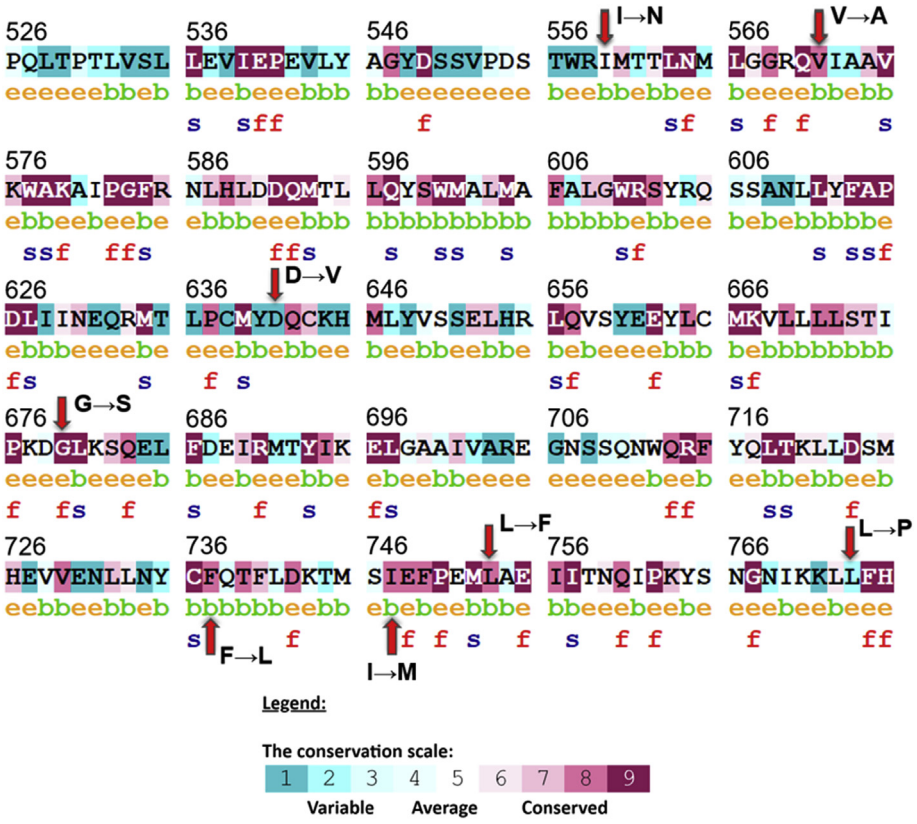

Fig. 2. Conservation analysis of the amino acids of the LBD 4P6W structure obtained by Consurf. Value 1 indicates high capacity for occurrence of amino acid exchanges. In contrast, value 9 indicates a high degree of conservation of the amino acid in the structure. Represented by red arrows are the SNPs that cause resistance to glucocorticoids: I559 N, V571A, D641V, G679S, F737L, I747 M, L753F and L773P. The letter "e" refers to an exposed residue according to the neural-network algorithm; "B" indicates a buried residue also according to the neural-network algorithm; "F" refers to a predicted as functional residue (highly conserved and exposed); "S" indicates a predicted structural residue (highly conserved and buried). (For interpretation of the references to color in this figure legend, the reader is referred to the Web version of this article.)

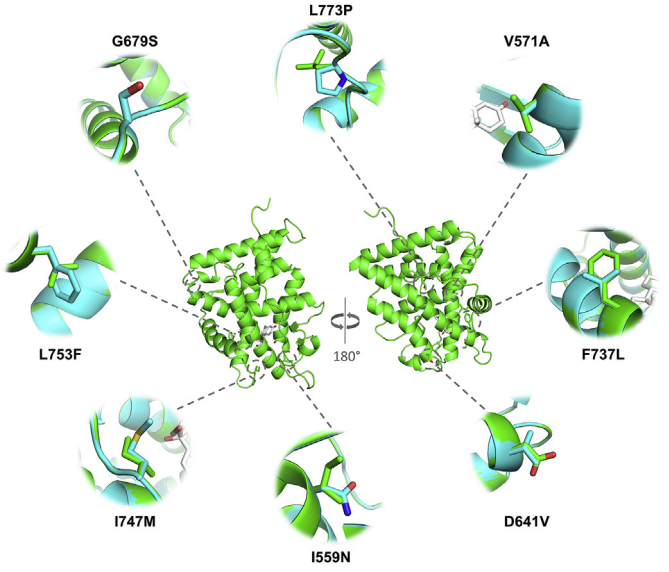

Fig. 3. Representation of wild-type and pathological SNPs models. The approximate images show the amino acid variant (in cyan) occurring in the GR structure when overlapped with the wild-type (green), shown only in its side chain; the cortisol molecule appears near to some mutations in white. In the center, the GR protein is found in its anterior plane (left) and, after 180° rotation of the Y axis, in the posterior plane (right). Table S2 shows the validation parameters. (For interpretation of the references to color in this figure legend, the reader is referred to the Web version of this article.)

ligand and receptor. According to the two-sided Wilcoxon-Mann-Whitney non-parametric test, seven out of eight mutations have differences compared to wild-type (p-value $< 2.2 \times 10^{-16}$). The exception is the I559 N mutation, which has exactly the same binding energy as wild-type (p-value $= 1$).

3.6. Mutations alter the structure of GR and impair cortisol binding to the receptor

Molecular dynamics simulation was performed from the complexes constructed through molecular docking of cortisol and the mutants or the wild-type GR LBD. The RMSD (Fig. 5A) was calculated to evaluate the difference in movement between the backbone of the wild-type GR protein and the variant structures. Fig. 5A showed that the trajectory of wild-type structure varied between 2 and 4 Å. The I559 N and L753F mutations demonstrated backbone alterations compared to the wild-type, with some oscillations slightly larger than 4 Å, as well as the F737L mutation, which showed structural variations between 3 and 5 Å. These results show that the receptor structure could present small modifications.

The RMSD is one option out of others to verify the structure similarity. From GROMACS built-in functions, no differences between wild-type and variants were observed for radius of gyration or for solvent accessible surface (data not shown). To confirm these results the TM-Score was applied as another measure of structural similarity. TM-Score showed that the mutant receptors have the same folding compared to the wild-type structure (Table 2). However, all structures, in the presence of variants, showed differences

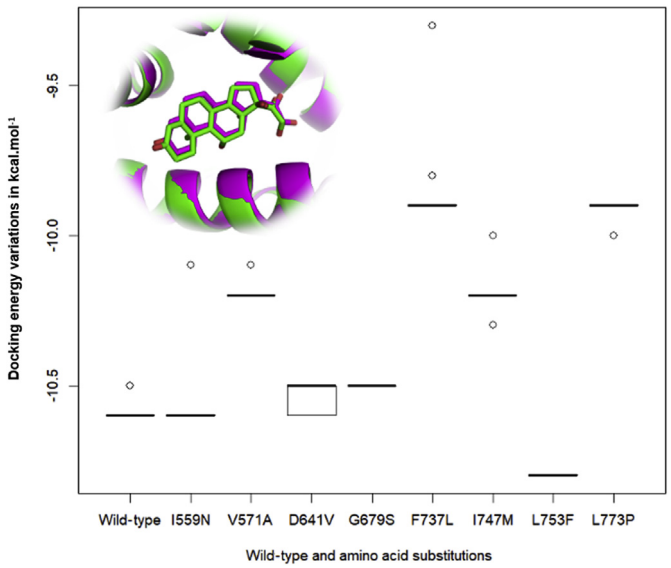

Fig. 4. Molecular docking of GR and cortisol ligand. In the top left, the cortisol molecule docking of the protein structure modeled (green) compared to the crystal structure (PDB ID 4P6X, in magenta). Boxplot shows the distribution of the energy values in kcal.mol^{-1} obtained from the binding of the cortisol molecule to the GR in wild-type models and mutations referring to the pathological SNPs. With a critical value of 0.05, all variants have differences compared to wild-type (p-value $< 2.2 \times 10^{-16}$). The exception is the I559 N mutation (p-value = 1). Given the fact that the ligand and receptor were set as rigid bodies, the majority of replicates generated the same result, which flattened the boxes to lines, except for D641V mutation which has a larger range of values allowing the sample division in the first quartile. The small circles represent outliers from the sample. (For interpretation of the references to color in this figure legend, the reader is referred to the Web version of this article.)

in the loop between α-helices 1 and 3 (referring to the binding site), and in the loop between α-helices 9 and 10, the region responsible for keeping the upper portion of the binding site stable. In addition, it was also observed that most of the mutant structures showed differences in the loop between α-helices 11 and AF-2, as well as in the α-helix AF-2 itself, whose regions have an important binding function with the co-activator GRIP1. Fig. 6 shows details of the amino acid substitutions compared to the wild-type, from the molecular dynamics analysis. The G679S, I747 M and L773P mutations, located in loops, present a larger structural modification in comparison to the other variants.

To evaluate the interaction of the GR receptor with the cortisol molecule during the simulation, the number of hydrogen bonds was computed between the residues of the GR pocket (Leu^{563}, by the carboxyl group of main chain; Asn^{564}; Gln^{570}; Arg^{611}; and Thr^{739}) and cortisol ligand. Compared to the wild-type, all mutations showed a decrease in hydrogen bonds, showing low interaction of the cortisol molecule at the binding site of the GR protein, especially the D641V, F737L, I747 M and L773P variants (Fig. 5B).

In order to analyze and visualize the overall movement of the GR protein structure and its variants, essential dynamics was performed. Fig. 7 demonstrates that the I559 N and I747 M variations did not show much difference in the flexibility of GR structure when compared to the native protein. However, the other variations showed less flexibility of the receptor.

4. Discussion

The glucocorticoid receptor promotes the binding of cortisol to the action of the hormone at the nucleus [55] (Fig. 1). The mutations analyzed here were previously evaluated *in vitro* and/or *in vivo* (Table 1), and although they do not have population frequency data, the results obtained could help to determine whether the changes that occur in more frequent variants could lead to functional losses of the receptor action mechanism [62].

According to the molecular docking analysis, all variants, with the exception of the L753F one, could present reduced affinity between receptor and ligand (Fig. 4), which is confirmed by the number of hydrogen bonds (Fig. 5B), indicating that there is a decrease in the receptor pocket's affinity for the cortisol ligand. This could explain the previously observed delayed translocation of the receptor-hormone complex to the nucleus [1,5,6,52,55,56], because the reduced affinity could inactivate the action of nuclear localization signals NL-1 and NL-2.

For the L753F mutation, an increased binding energy (-10.8 kcal mol^{-1}) compared to wild-type (-10.6 kcal mol^{-1}) was observed (Fig. 4). A previous report showed that cortisol could bind to the L753F variant in a non-physiological condition (at 4 °C) [61]. As the temperature is not completely simulated by molecular docking, this experiment suggested the ligand permanence at GR LBD structure. However, molecular dynamics is one solution among others to overcome this bias, as the temperature could be simulated. On such simulation the number of hydrogen bonds showed decreased cortisol-receptor interaction at 37 °C, being in alignment with the literature data [60,61].

The binding to cortisol is only the first step of the GR action mechanism, in which the next steps may still occur. Several studies show that these eight variants could interfere with the functional activity of the subdomain AF-2, leading to inadequate interaction with GRIPs [1,6,55–57,60], and this may be related to the structural modifications caused by the variations.

The RMSD analysis (Fig. 5A) showed small structural modifications of I559 N, V571A, D641V and L773P variants, as well as the essential dynamics analysis (Fig. 7), which exhibited the mutated structure with few changes of flexibility, maintaining the movement of the protein, when compared to the wild-type. On the other hand, the V571A mutation was seen to cause a higher change in the flexibility of the GR structure, presented in the essential dynamics. Furthermore, in RMSD analysis, the L753F mutation also indicated a variation between 3.5 and 4.5 Å, as well as the essential dynamics that demonstrated a low receptor movement when compared to the wild-type.

The Leu^{773} residue, in the downstream region of the AF-2 α-helix, confers structural stability and maintains the conformation of the GR LBD domain, by means of the interaction between the α-helices 8, 9, 10 and the AF-2 α-helix itself, for the binding of the molecule cortisol under normal conditions. The L773P mutation could destabilize the interaction between those α-helices (Fig. 6), which could reflect the possible reduced affinity to cortisol (Fig. 4). This low affinity may also result in inactivating the NL-2 nuclear localization signal, delaying the translocation of the protein to the nucleus. The NL-1 signal may also have an impaired role because the mutation prevents allosteric conformation of the receptor (induced by cortisol binding), also causing delay in nuclear translocation [1].

Essential dynamics analysis showed a less flexible behavior in the G679S (Fig. 7D) and F737L (Fig. 7E) mutant receptor structures. Furthermore, the F737L variant presented structural instability, observed in the RMSD backbone analysis (Fig. 5A), varying between 3 and 5 Å in the backbone movement, compared to the wild-type, which oscillated between 3 and 4 Å.

The G679S mutation is in an important location for the maintenance of α-helices 8 and 9, which maintains the binding site stable for receptor-cortisol interaction. This mutation occurs in the conserved region of β-strand leading to the destabilization of α-helices 8 and 9, which could cause instability at the binding site and

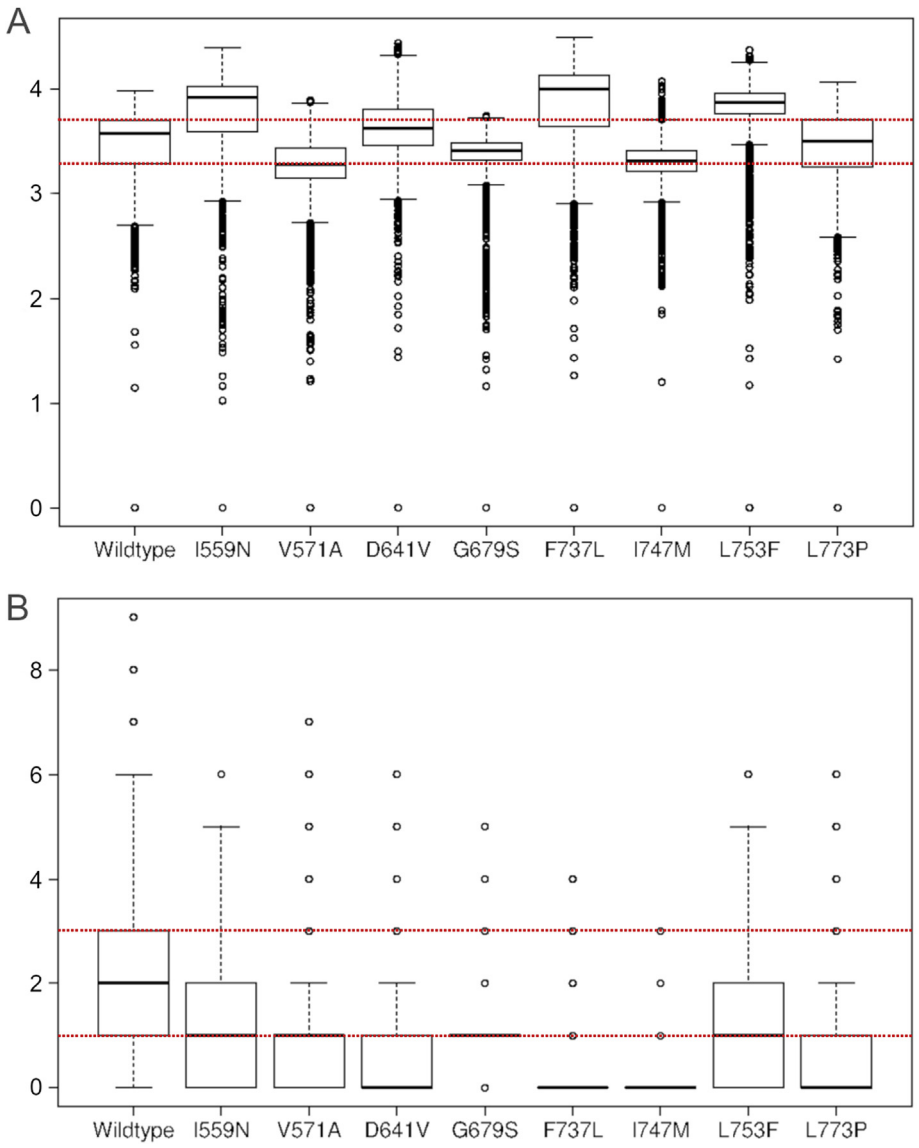

Fig. 5. GR protein and variants' trajectory analyses plotted in boxplots. (A) Backbone RMSD and, (B) number of hydrogen bonds of wild-type and variants. The backbone RMSD (A) values are in Å. Dotted red lines on plots indicate the reference values of wild-type. (For interpretation of the references to color in this figure legend, the reader is referred to the Web version of this article.)

Table 2
Structural similarity summary of results obtained from the TM-Score server. Values of tm-score above 0.5 indicate that the two compared structures share the same folding.

Mutations	RMSD(Å)[a]	TM-score[a]
p.I559 N	3.424	0.8001
p.V571A	4.005	0.8258
p.D641V	3.631	0.7875
p.G679S	4.058	0.8399
p.F737L	3.361	0.7929
p.I747 M	3.697	0.8412
p.L753F	3.413	0.7815
p.L773P	4.174	0.7838

[a] Data generated by comparing the wild-type structure with mutant receptor at 200ns. The PDB Structures are available in the supplementary information.

could reduce the cortisol receptor affinity [55]. On the other hand, F737L mutation may reduce the affinity to cortisol due to the location of the mutation in the α-helix 11, which integrates the back region of the receptor-binding pocket (Fig. 7), maintaining the integrity of the site so that the binding of the glucocorticoid to the GR LBD occurs correctly [56].

The Ile^{747} residue is located in the loop between α-helices 11 and AF-2. This residue could also interfere with the stability of the binding site, causing a possible affinity reduction and receptor-ligand instability in the two α-helices, 11 and AF-2, responsible for maintaining the integrity of the ligand-pocket [57].

The location of the I747 M seems to distort the binding between the receptor and cortisol, which could result in impairment of the dissociation of the heat shock proteins, which in turn may delay the nuclear translocation process [6].

Indeed, when checking structural similarity, all mutants were observed to share the same folding as wild-type, by means of the TM-Score analysis (Table 2). Even so, the variant structures had regions of misalignment that are important for the execution of the GR action mechanism, such as (i) the loop between α-helices 1 and 3 that constitute the cortisol binding site; (ii) the loop between α-helices 11 and AF-2, as well as the AF-2 α-helix itself, regions of

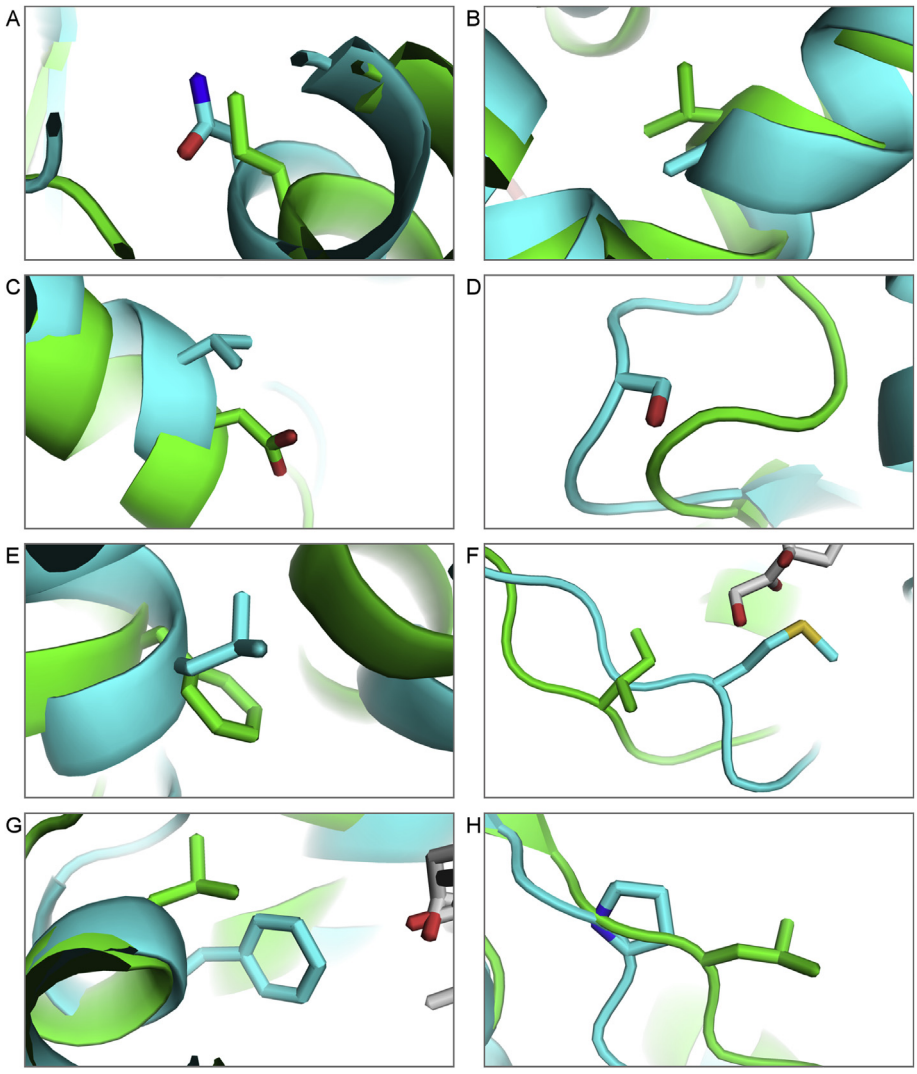

Fig. 6. Detail of amino acid substitutions (in cyan) aligned to the wild-type (green) structure of the receptor, from molecular dynamics. (A) I559 N mutation; (B) V571A; in (C) D641V; (D) G679S; (E) F737L; (F) I747 M; (G) L753F; (H) L773P. The structures' snapshots were obtained in 200ns of the simulation. The cortisol molecule, in white, appears close to the I747 M and L753F mutations. The structures were aligned using Pymol. (For interpretation of the references to color in this figure legend, the reader is referred to the Web version of this article.)

interaction with the co-activator GRIP; and (iii) the loop between α-helices 9 and 10, which maintains the upper portion of the binding site. Therefore, the action mechanism is impaired not only by the reduction of cortisol affinity, but also by a number of structural changes.

Since the GR action mechanism comprises several steps, the lack of the entire complex depicted in Fig. 1 is a limitation of the present work. Therefore, we have to be careful with some results, as the simulations do not include the co-activator GRIP1 (as it does not have a complete structure solved), and its interaction with the receptor has a strong influence on the activity of the GR mechanism [6]. However, even using a partial complex, there are some useful information that could be retrieved, as demonstrated by Chitrala et al. [19]; Pires et al. [13]; and Muthusamy & Naganami [26], which also used partial complexes to gain insight about mutation effects on protein structure. Henceforth, this study may impel further subsequent analyses on the AF-1 and AF-2 transactivation subdomains and the GR activity within the nucleus with the investigation of the DNA binding domain. In this context, further analyses that include the DNA binding and transactivation domains are also desirable to better understand the cascade of events that cause the phenotypic manifestations of this pathology.

5. Conclusion

The study of mutations that are known to cause glucocorticoid resistance makes it possible to understand the structural changes that result in pathological response in the organism. The action mechanism of glucocorticoid resistance comprises several events until the disease is manifested by the phenotype characteristic. Here, we observed changes in the structure of the LBD domain of GR, which trigger effects that could lead to the emergence of glucocorticoid resistance in different stages, especially cortisol binding, translocation of the receptor-hormone complex to the nucleus and its interaction with co-activator GRIP1. The variants analyzed cause structural alterations and a decrease in the affinity between the cortisol molecule and the pocket of mutant receptors. Finally, molecular dynamics analyses provided evidence about the behavior of the GR structure, clarifying the changes that led to the structural instability of the receptor in the presence of the mutations, modifying important loops and α-helices, interfering with the GR action mechanism, and culminating in the glucocorticoid

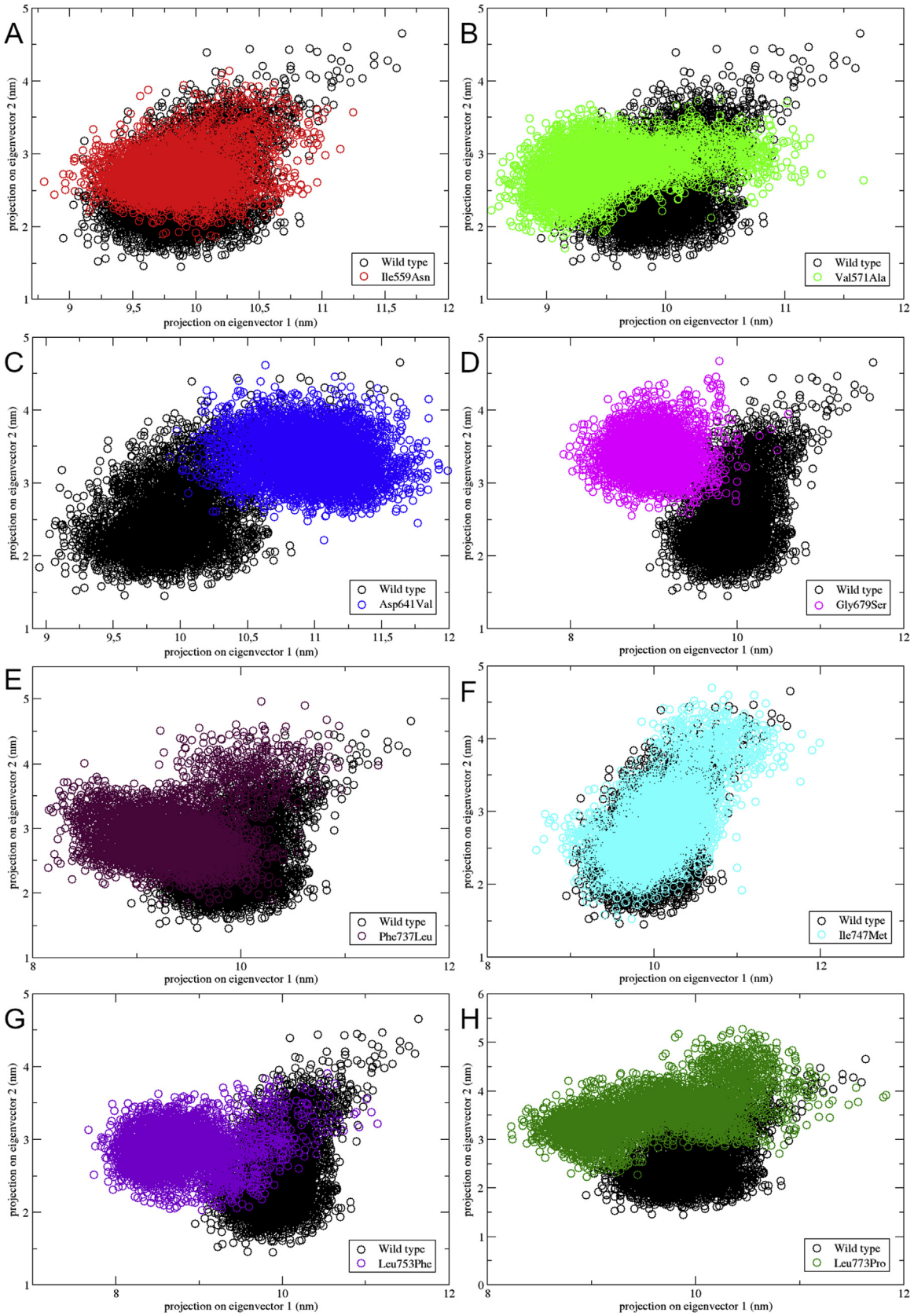

Fig. 7. Projection of the motion of GR protein in phase space along the first two principal eigenvectors. The black circles represent the native wild-type GR and the other color circles the variants as follows: I559 N (A), V571A (B), D641V (C), G679S (D), F737L (E), I747 M (F), L753F (G) and L773P (H). I559 N and D641V variants had a smallest difference in flexibility compared to wild-type. However, the other variations showed lower receptor flexibility when compared to the native protein. (For interpretation of the references to color in this figure legend, the reader is referred to the Web version of this article.)

resistance phenotype. In future studies, the data here reported could be used as a control for modelling other mutations that have not been evaluated by *in vitro* or *in vivo* techniques, accelerating the discovery of new mutations that could result in glucocorticoid resistance.

Acknowledgements

This work was supported by Conselho Nacional de Desenvolvimento Científico e Tecnológico (CNPq), Coordenação de Aperfeiçoamento de Pessoal do Nível Superior (CAPES), Fundação de Amparo à Pesquisa do Distrito Federal (FAPDF) and Fundação de Apoio ao Desenvolvimento do Ensino, Ciência e Tecnologia do Estado de Mato Grosso do Sul (FUNDECT).

Appendix A. Supplementary data

Supplementary data to this article can be found online at https://doi.org/10.1016/j.jmgm.2019.07.020.

References

[1] E. Charmandari, A. Raji, T. Kino, T. Ichijo, A. Tiulpakov, K. Zachman, G.P. Chrousos, A novel point mutation in the ligand-binding domain (LBD) of the human glucocorticoid receptor (hGR) causing generalized glucocorticoid resistance: the importance of the C terminus of hGR LBD in conferring transactivational activity, J. Clin. Endocrinol. Metab. 90 (2005) 3696–3705, https://doi.org/10.1210/jc.2004-1920.

[2] B.M. Necela, J.A. Cidlowski, A single amino acid change in the first zinc finger of the DNA binding domain of the glucocorticoid receptor regulates differential promoter selectivity, J. Biol. Chem. 279 (2004) 39279–39288, https://doi.org/10.1074/jbc.M405489200.

[3] S. Checkley, The neuroendocrinology of depression and chronic stress, Br. Med. Bull. 52 (1996) 597–617, https://doi.org/10.1093/oxfordjournals.bmb.a011570.

[4] R.K. Bledsoe, V.G. Montana, T.B. Stanley, C.J. Delves, C.J. Apolito, D.D. McKee, T.G. Consler, D.J. Parks, E.L. Stewart, T.M. Willson, M.H. Lambert, J.T. Moore, K.H. Pearce, H.E. Xu, Crystal structure of the glucocorticoid receptor ligand binding domain reveals a novel mode of receptor dimerization and coactivator recognition, Cell 110 (2002) 93–105, https://doi.org/10.1016/S0092-8674(02)00817-6.

[5] B.B. Mendonca, M.V. Leite, M. de Castro, T. Kino, L.L.K. Elias, T.A.S. Bachega, I.J.P. Arnhold, G.P. Chrousos, A.C. Latronico, Female pseudohermaphroditism caused by a novel homozygous missense mutation of the GR gene, J. Clin. Endocrinol. Metab. 87 (2002) 1805–1809, https://doi.org/10.1210/jcem.87.4.8379.

[6] E. Charmandari, T. Kino, E. Souvatzoglou, A. Vottero, N. Bhattacharyya, G.P. Chrousos, Natural glucocorticoid receptor mutants causing generalized glucocorticoid resistance: molecular genotype, genetic transmission, and clinical phenotype, J. Clin. Endocrinol. Metab. 89 (2004) 1939–1949, https://doi.org/10.1210/jc.2003-030450.

[7] M.R. Yudt, J.A. Cidlowski, Molecular identification and characterization of A and B forms of the glucocorticoid receptor, Mol. Endocrinol. 15 (2001) 1093–1103, https://doi.org/10.1210/mend.15.7.0667.

[8] D. Ratman, W. Vanden Berghe, L. Dejager, C. Libert, J. Tavernier, I.M. Beck, K. De Bosscher, How glucocorticoid receptors modulate the activity of other transcription factors: a scope beyond tethering, Mol. Cell. Endocrinol. 380 (2013) 41–54, https://doi.org/10.1016/j.mce.2012.12.014.

[9] P.J. Ballester, J.B.O. Mitchell, A machine learning approach to predicting protein–ligand binding affinity with applications to molecular docking, Bioinformatics 26 (2010) 1169–1175, https://doi.org/10.1093/bioinformatics/btq112.

[10] D.K. Brown, Ö. Tastan Bishop, Role of structural bioinformatics in drug discovery by computational SNP analysis. A proposed protocol for analyzing variation at the protein level, Glob. Heart. (2017) 1–11, https://doi.org/10.1016/j.gheart.2017.01.009.

[11] W.F. Porto, F.A. Marques, H.B. Pogue, M.T. de Oliveira Cardoso, M.G.R. do Vale, Á. da Silva Pires, O.L. Franco, S.A. de Alencar, R. Pogue, Computational investigation of growth hormone receptor Trp169Arg heterozygous mutation in a child with short stature, J. Cell. Biochem. 118 (2017) 4762–4771, https://doi.org/10.1002/jcb.26144.

[12] M. Karplus, J. Kuriyan, Molecular dynamics and protein function, Proc. Natl. Acad. Sci. U. S. A 102 (2005) 6679–6685, https://doi.org/10.1073/pnas.0408930102.

[13] A.S. Pires, W.F. Porto, O.L. Franco, S.A. Alencar, In silico analyses of deleterious missense SNPs of human apolipoprotein E3, Sci. Rep. 7 (2017) 2509, https://doi.org/10.1038/s41598-017-01737-w.

[14] A. Kumar, R. Purohit, Use of long term molecular dynamics simulation in predicting cancer associated SNPs, PLoS Comput. Biol. 10 (2014), https://doi.org/10.1371/journal.pcbi.1003318 e1003318.

[15] G. Tanwar, R. Purohit, Gain of native conformation of Aurora A S155R mutant by small molecules, J. Cell. Biochem. 120 (2019) 11104–11114, https://doi.org/10.1002/jcb.28387.

[16] P. Arezi, Z. Rezvani, The variation of mitochondrial NADH dehydrogenase subunit 4 (mtND4) and molecular dynamics simulation of SNPs among Iranian women with breast cancer, J. Mol. Graph. Model. 85 (2018) 242–249, https://doi.org/10.1016/J.JMGM.2018.08.011.

[17] V. Rajendran, C. Gopalakrishnan, R. Purohit, Impact of point mutation P29S in RAC1 on tumorigenesis, Tumor Biol. 37 (2016) 15293–15304, https://doi.org/10.1007/s13277-016-5329-y.

[18] V. Bhardwaj, R. Purohit, Computational investigation on effect of mutations in PCNA resulting in structural perturbations and inhibition of mismatch repair pathway, J. Biomol. Struct. Dyn. (2019) 1–12, https://doi.org/10.1080/07391102.2019.1621210.

[19] K.N. Chitrala, S. Yeguvapalli, Computational screening and molecular dynamic simulation of breast cancer associated deleterious non-synonymous single nucleotide polymorphisms in TP53 gene, PLoS One 9 (2014) e104242, https://doi.org/10.1371/journal.pone.0104242.

[20] W.F. Porto, O.L. Franco, S.A. Alencar, Computational analyses and prediction of guanylin deleterious SNPs, Peptides 69 (2015) 92–102, https://doi.org/10.1016/j.peptides.2015.04.013.

[21] A.C.S. Marcolino, W.F. Porto, Á.S. Pires, O.L. Franco, S.A. Alencar, Structural impact analysis of missense SNPs present in the uroguanylin gene by long-term molecular dynamics simulations, J. Theor. Biol. 410 (2016) 9–17, https://doi.org/10.1016/j.jtbi.2016.09.008.

[22] Á.S. Pires, W.F. Porto, P.O. Castro, O.L. Franco, S.A. Alencar, Theoretical structural characterization of lymphoguanylin: a potential candidate for the development of drugs to treat gastrointestinal disorders, J. Theor. Biol. 419 (2017) 193–200, https://doi.org/10.1016/j.jtbi.2017.02.016.

[23] W.F. Porto, D.O. Nolasco, Állan S. Pires, R.W. Pereira, O.L. Franco, S.A. Alencar, Á.S. Pires, R.W. Pereira, O.L. Franco, S.A. Alencar, Prediction of the impact of coding missense and nonsense single nucleotide polymorphisms on HD5 and HBD1 antibacterial activity against Escherichia coli, Biopolymers 106 (2016) 633–644, https://doi.org/10.1002/bip.22866.

[24] W.F. Porto, D.O. Nolasco, Á.S. Pires, G.R. Fernandes, O.L. Franco, S.A. Alencar, HD5 and HBD1 variants' solvation potential energy correlates with their antibacterial activity against Escherichia coli, Biopolymers 106 (2016) 43–50, https://doi.org/10.1002/bip.22763.

[25] B. Righino, A. Minucci, D. Pirolli, E. Capoluongo, G. Conti, D. De Luca, M.C. De Rosa, In silico investigation of the molecular effects caused by R123H variant in secretory phospholipase A2-IIA associated with ARDS, J. Mol. Graph. Model. 81 (2018) 68–76, https://doi.org/10.1016/J.JMGM.2018.02.014.

[26] K. Muthusamy, S. Nagamani, Vitamin D receptor (VDR) non-synonymous single nucleotide polymorphisms (nsSNPs) affect the calcitriol drug response - a theoretical insight, J. Mol. Graph. Model. 81 (2018) 14–24, https://doi.org/10.1016/J.JMGM.2018.02.004.

[27] P. Sang, W. Hu, Y.-J. Ye, L.-H. Li, C. Zhang, Y.-H. Xie, Z.-H. Meng, In silico screening, molecular docking, and molecular dynamics studies of SNP-derived human P5CR mutants, J. Biomol. Struct. Dyn. 35 (2017) 2441–2453, https://doi.org/10.1080/07391102.2016.1222967.

[28] H. Ashkenazy, S. Abadi, E. Martz, O. Chay, I. Mayrose, T. Pupko, N. Ben-Tal, ConSurf, An improved methodology to estimate and visualize evolutionary conservation in macromolecules, Nucleic Acids Res. 44 (2016) W344–W350, https://doi.org/10.1093/nar/gkw408, 2016.

[29] G. Celniker, G. Nimrod, H. Ashkenazy, F. Glaser, E. Martz, I. Mayrose, T. Pupko, N. Ben-Tal, ConSurf: using evolutionary data to raise testable hypotheses about protein function, Isr. J. Chem. 53 (2013) 199–206, https://doi.org/10.1002/ijch.201200096.

[30] C. Angermüller, A. Biegert, J. Söding, Discriminative modelling of context-specific amino acid substitution probabilities, Bioinformatics 28 (2012) 3240–3247, https://doi.org/10.1093/bioinformatics/bts622.

[31] B.E. Suzek, H. Huang, P. McGarvey, R. Mazumder, C.H. Wu, UniRef: comprehensive and non-redundant UniProt reference clusters, Bioinformatics 23 (2007) 1282–1288, https://doi.org/10.1093/bioinformatics/btm098.

[32] Y. Dehouck, J.M. Kwasigroch, D. Gilis, M. Rooman, PoPMuSiC 2.1: a web server for the estimation of protein stability changes upon mutation and sequence optimality, BMC Bioinf. 12 (2011) 151, https://doi.org/10.1186/1471-2105-12-151.

[33] C.L. Worth, R. Preissner, T.L. Blundell, SDM–a server for predicting effects of mutations on protein stability and malfunction, Nucleic Acids Res. 39 (2011) W215–W222, https://doi.org/10.1093/nar/gkr363.

[34] J. Schymkowitz, J. Borg, F. Stricher, R. Nys, F. Rousseau, L. Serrano, The FoldX web server: an online force field, Nucleic Acids Res. 33 (2005) W382–W388, https://doi.org/10.1093/nar/gki387.

[35] F. Pucci, R.R. Bourgeas, M. Rooman, Predicting protein thermal stability changes upon point mutations using statistical potentials: introducing HoTMuSiC, Sci. Rep. 6 (2016) 23257, https://doi.org/10.1038/srep23257.

[36] F. Ancien, F. Pucci, M. Godfroid, M. Rooman, Prediction and interpretation of deleterious coding variants in terms of protein structural stability, Sci. Rep. (2018), https://doi.org/10.1038/s41598-018-22531-2.

[37] N. Eswar, B. Webb, M.A. Marti-Renom, M.S. Madhusudhan, D. Eramian, M.-Y. Shen, U. Pieper, A. Sali, Comparative protein structure modeling using modeller, Curr. Protoc. Bioinformatics 5 (2006), https://doi.org/10.1002/

0471250953.bi0506s15. Unit-5.6.
[38] M. Wiederstein, M.J. Sippl, ProSA-web: interactive web service for the recognition of errors in three-dimensional structures of proteins, Nucleic Acids Res. 35 (2007) W407–W410, https://doi.org/10.1093/nar/gkm290.
[39] R.A. Laskowski, M.W. MacArthur, D.S. Moss, J.M. Thornton, PROCHECK: a program to check the stereochemical quality of protein structures, J. Appl. Crystallogr. 26 (1993) 283–291, https://doi.org/10.1107/S0021889892009944.
[40] O. Trott, A.J. Olson, AutoDock Vina, Improving the speed and accuracy of docking with a new scoring function, efficient optimization, and multithreading, J. Comput. Chem. 31 (2009), https://doi.org/10.1002/jcc.21334. NA-NA.
[41] G.M. Morris, R. Huey, W. Lindstrom, M.F. Sanner, R.K. Belew, D.S. Goodsell, A.J. Olson, AutoDock4 and AutoDockTools4: automated docking with selective receptor flexibility, J. Comput. Chem. 30 (2009) 2785–2791, https://doi.org/10.1002/jcc.21256.
[42] Y. He, W. Yi, K. Suino-Powell, X.E. Zhou, W.D. Tolbert, X. Tang, J. Yang, H. Yang, J. Shi, L. Hou, H. Jiang, K. Melcher, H.E. Xu, Structures and mechanism for the design of highly potent glucocorticoids, Cell Res. 24 (2014) 713–726, https://doi.org/10.1038/cr.2014.52.
[43] H.J.C. Berendsen, J.P.M. Postma, W.F. van Gunsteren, J. Hermans, Interaction models for water in relation to protein hydration, in: B. Pullman (Ed.), Intermol. Forces, Springer, 1981, pp. 331–338.
[44] G.T. Ibragimova, R.C. Wade, Importance of explicit salt ions for protein stability in molecular dynamics simulation, Biophys. J. 74 (1998) 2906–2911, https://doi.org/10.1016/S0006-3495(98)77997-4.
[45] B. Hess, C. Kutzner, D. van der Spoel, E. Lindahl, GROMACS 4: algorithms for highly efficient, load-balanced, and scalable molecular simulation, J. Chem. Theory Comput. 4 (2008) 435–447, https://doi.org/10.1021/ct700301q.
[46] A.W. Schüttelkopf, D.M.F. van Aalten, PRODRG: a tool for high-throughput crystallography of protein-ligand complexes, Acta Crystallogr. Sect. D Biol. Crystallogr. 60 (2004) 1355–1363, https://doi.org/10.1107/S0907444904011679.
[47] S. Miyamoto, P.A. Kollman, Settle: an analytical version of the SHAKE and RATTLE algorithm for rigid water models, J. Comput. Chem. 13 (1992) 952–962, https://doi.org/10.1002/jcc.540130805.
[48] B. Hess, H. Bekker, H.J.C. Berendsen, J.G.E.M. Fraaije, LINCS: a linear constraint solver for molecular simulations, J. Comput. Chem. 18 (1997) 1463–1472, https://doi.org/10.1002/(SICI)1096-987X(199709)18:12<1463::AID-JCC4>3.0.CO;2-H.
[49] T. Darden, D. York, L. Pedersen, Particle mesh Ewald: an N·log(N) method for Ewald sums in large systems, J. Chem. Phys. 98 (1993) 10089, https://doi.org/10.1063/1.464397.
[50] Y. Zhang, J. Skolnick, Scoring function for automated assessment of protein structure template quality, Proteins 57 (2004) 702–710, https://doi.org/10.1002/prot.20264.
[51] J. Xu, Y. Zhang, How significant is a protein structure similarity with TM-score = 0.5? Bioinformatics 26 (2010) 889–895, https://doi.org/10.1093/bioinformatics/btq066.
[52] M. Ruiz, U. Lind, M. Gafvels, G. Eggertsen, J. Carlstedt-Duke, L. Nilsson, M. Holtmann, P. Stierna, A.-C. Wikstrom, S. Werner, Characterization of two novel mutations in the glucocorticoid receptor gene in patients with primary cortisol resistance, Clin. Endocrinol. 55 (2001) 363–371, https://doi.org/10.1046/j.1365-2265.2001.01323.x.
[53] T. Kino, R.H. Stauber, J.H. Resau, G.N. Pavlakis, G.P. Chrousos, Pathologic human GR mutant has a transdominant negative effect on the wild-type GR by inhibiting its translocation into the nucleus: importance of the ligand-binding domain for intracellular GR trafficking, J. Clin. Endocrinol. Metab. 86 (2001) 5600–5608, https://doi.org/10.1210/jcem.86.11.8017.
[54] D.M. Hurley, D. Accili, C.A. Stratakis, M. Karl, N. Vamvakopoulos, E. Rorer, K. Constantine, S.I. Taylor, G.P. Chrousos, Point mutation causing a single amino acid substitution in the hormone binding domain of the glucocorticoid receptor in familial glucocorticoid resistance, J. Clin. Investig. 87 (1991) 680–686, https://doi.org/10.1172/JCI115046.
[55] E. Charmandari, T. Kino, T. Ichijo, K. Zachman, A. Alatsatianos, G.P. Chrousos, Functional characterization of the natural human glucocorticoid receptor (hGR) mutants hGRαR477H and hGRαG679S associated with generalized glucocorticoid resistance, J. Clin. Endocrinol. Metab. 91 (2006) 1535–1543, https://doi.org/10.1210/jc.2005-1893.
[56] E. Charmandari, T. Kino, T. Ichijo, W. Jubiz, L. Mejia, K. Zachman, G.P. Chrousos, A novel point mutation in helix 11 of the ligand-binding domain of the human glucocorticoid receptor gene causing generalized glucocorticoid resistance, J. Clin. Endocrinol. Metab. 92 (2007) 3986–3990, https://doi.org/10.1210/jc.2006-2830.
[57] A. Vottero, T. Kino, H. Combe, P. Lecomte, G.P. Chrousos, A novel, C-terminal dominant negative mutation of the GR causes familial glucocorticoid resistance through abnormal interactions with p160 steroid receptor coactivators, J. Clin. Endocrinol. Metab. 87 (2002) 2658–2667, https://doi.org/10.1210/jcem.87.6.8520.
[58] J. Ashraf, E.B. Thompson, Identification of the activation-labile gene: a single point mutation in the human glucocorticoid receptor presents as two distinct receptor phenotypes, Mol. Endocrinol. 7 (1993) 631–642, https://doi.org/10.1210/mend.7.5.8316249.
[59] A.G. Hillmann, J. Ramdas, K. Multanen, M.R. Norman, J.M. Harmon, Glucocorticoid receptor gene mutations in leukemic cells acquired in vitro and in vivo, Cancer Res. 60 (2000) 2056–2062.
[60] J.H. Powers, A.G. Hillmann, D.C. Tang, J.M. Harmon, Cloning and expression of mutant glucocorticoid receptors from glucocorticoid-sensitive and -resistant human leukemic cells, Cancer Res. 53 (1993) 4059–4065.
[61] L.A. Palmer, J.M. Harmon, Biochemical evidence that glucocorticoid-sensitive cell lines derived from the human leukemic cell line CCRF-CEM express a normal and a mutant glucocorticoid receptor gene, Cancer Res. 51 (1991) 5224–5231.
[62] C.S. Martins, D. Elias, L.M. Colli, C.E. Couri, M.C.L.A. Souza, A.C. Moreira, M.C. Foss, L.L.K. Elias, M. de Castro, HPA axis dysregulation, *NR3C1* polymorphisms and glucocorticoid receptor isoforms imbalance in metabolic syndrome, Diabetes Metabol. Res. Rev. 33 (2017) e2842, https://doi.org/10.1002/dmrr.2842.